ANALYSIS OF CIRCULAR MICROSTRIP ANTENNA ON THICK SUBSTRATE

A. K. Verma and Nasimuddin
Department of Electronic Science
University of Delhi South Campus, New Delhi-110021, INDIA

Abstract

An improved cavity model called the modified Wolff model (MWM) is presented to compute the resonance frequency, input impedance and bandwidth of the circular microstrip antenna on thick substrate (substrate thickness, $0.003\lambda_g$–$0.1\lambda_g$). The results of MWM show better agreement with the experimental results as compared to the results of three commercial software, including the method of moment (MOM) based Ensemble. The MWM provides deviation in resonance frequency within 1.69 % and deviation in resonant resistance within 17 % against the experimental results.

Indexing terms: Microstrip antennas, Thick substrate, Circular microstrip antennas

I. INTRODUCTION

An improved version of the cavity model, called the modified Wolff model (MWM) was reported to compute accurately resonance frequency of the circular microstrip antenna on the lossless substrate [1]. In this work we extend the MWM for computation of resonance frequency, bandwidth and input impedance of the probe fed circular patch on the thick lossy substrate. These parameters of the circular patch on thick substrate are computed by the field theoretic methods and the standard cavity model is not considered accurate [2]. We have collected the experimental results from the seven published sources [2-8] for the substrate thickness between $0.003\lambda_g$ – $0.1\lambda_g$. The λ_g is the guided wavelength in the dielectric medium. We have used these data to compare the computed results obtained by the present MWM and also by three commercial software namely, the MOM based Ensemble [9], the standard cavity model adopted in the PCAAD by Pozar [10] and the multiport cavity model (MCM) adopted in the Micropatch by Benalla et al.[11] against the common experimental results. In all cases, the results of MWM are much closer to the experimental results as compared to the computed results of these commercial software.

II. MODIFIED WOLFF MODEL

The rectangular and circular microstrip patch antenna fabricated on the same substrate (ε_r = 2.32, h = 0.159 cm) and at the same resonant frequency (f_r = 2 GHz) provide almost same directivity (7 dB) and efficiency (91%) [12]. This identical performance suggests that the circular microstrip

Copyright SBMO ISSN 1516-7399

patch antenna can be analyzed by obtaining an equivalent rectangular microstrip patch antenna. The circular patch and its equivalent rectangular patch is shown in Fig.1.

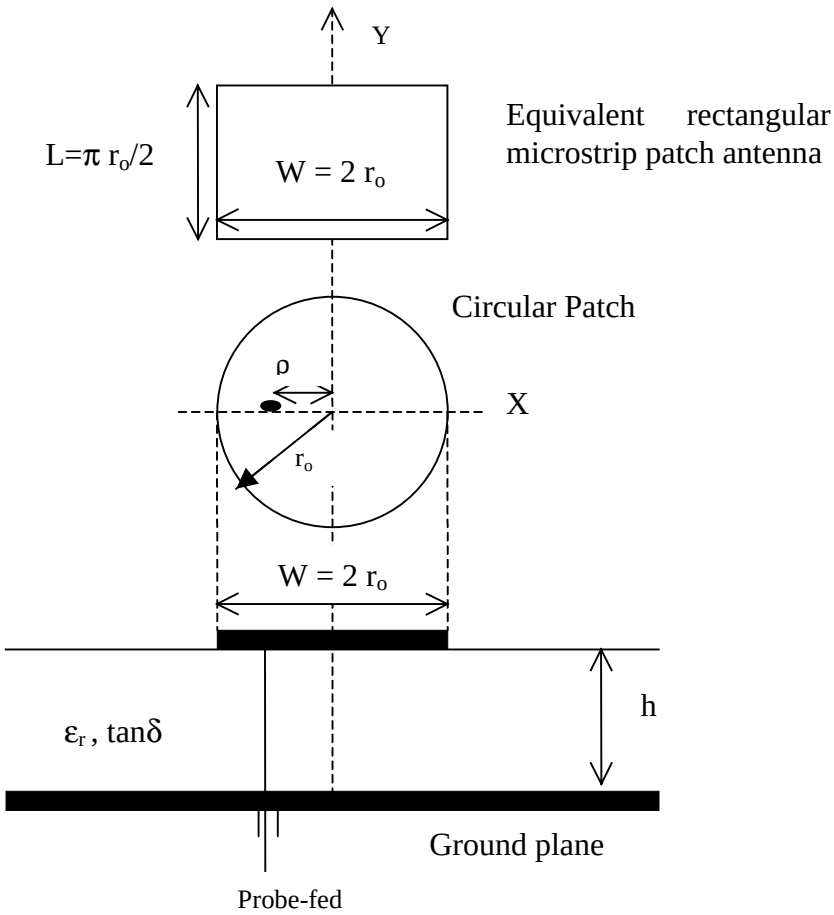

Fig. 1. Circular patch antenna and its equivalent rectangular patch antenna on thick substrate.

For the equivalent rectangular patch of width $W = 2r_o$, the length $L = (\pi/2)r_o$ is obtained by using the invariance of electrostatic energy below both the rectangular and circular patches. The fringe capacitance computed along both the length sides of the equivalent rectangular patch is treated same as the fringe capacitance of the original circular patch. The resonance frequency of the circular microstrip antenna on thick lossy substrate is computed from [1],

$$f_r = \mathrm{Re}\left[\frac{V_0 \alpha_{nm}}{2\pi r_{eff}\sqrt{\varepsilon^*_{r\,dyn}}}\right] \tag{1}$$

For the fundamental resonating TM_{11} mode, $\alpha_{nm} = 1.841$. V_0 is the velocity of light. The effective radius r_{eff} is computed by the expression of Chew and Kong [13],

$$r_{eff} = r_o\left[1+\frac{2h}{\pi r_o\,\varepsilon_r^{/}}\left\{\ln\left(\frac{r_o}{2h}\right)+\left(1.41\varepsilon_r^{/}+1.77\right)+\frac{h}{r_o}\left(0.268\varepsilon_r^{/}+1.65\right)\right\}\right]^{\frac{1}{2}} \tag{2}$$

where r_o is radius of the patch, h is height of the substrate and $\varepsilon_r^{/}$ is real part of complex relative permittivity (ε_r^*) of the substrate. The complex dynamic relative permittivity of the circular patch, which takes into account the fringe field and modal field variation, is obtained from,

$$\varepsilon^*_{r\,dyn} = \frac{C^*_{dyn}\left(\varepsilon_r^*, h, 2r_o\right)}{C_{dyn}\left(\varepsilon_r = 1, h, 2r_o\right)} \tag{3}$$

The total mode-dependent complex dynamic capacitance $C^*_{dyn}\left(\varepsilon_r^*, h, 2r_o\right)$ of the circular patch is computed by the variational method in the Fourier domain, where real ε_r is replaced by the complex ε_r^* [1].

The frequency dependent input impedance of the probe fed circular microstrip patch is determined by the following equation of a parallel resonant circuit [14],

$$Z_{in}(f) = \frac{R(\rho)}{1+Q_T^2\left[\frac{f}{f_r}-\frac{f_r}{f}\right]} + j\left[X_L - \frac{R(\rho)\,Q_T\left[\frac{f}{f_r}-\frac{f_r}{f}\right]}{1+Q_T^2\left[\frac{f}{f_r}-\frac{f_r}{f}\right]^2}\right] \tag{4}$$

The input resistance at the feed point ρ from the center of the circular patch is given by,

$$R(\rho) = \frac{1}{G_T}\frac{J_1^2(K\rho)}{J_1^2(K r_o)} \tag{5}$$

For the fundamental TM_{11} mode, K r_o equals to 1.84118 and G_T is the total conductance of the radiating aperture due to the conductor, dielectric, surface wave and radiation losses. At the resonant frequency f_r, it is related to the total Q-factor (Q_T) by,

$$G_T = G_R + G_D + G_C + G_{SW} = \left(\frac{2.39}{4\mu_o h f_r}\right)\frac{1}{Q_T} \tag{6}$$

and,

$$\frac{1}{Q_T} = \frac{1}{Q_C} + \frac{1}{Q_D} + \frac{1}{Q_{SW}} + \frac{1}{Q_R} \tag{7}$$

where Q_D, Q_C, Q_{SW}, and Q_R are the Q- factors, due to dielectric loss, conductor loss (in patch, ground plane and in the co-axial feed), surface-wave loss and radiation loss respectively. For the equivalent rectangular patch of width, W = $2r_o$ the Q_D is determined from,

Copyright SBMO ISSN 1516-7399

$$Q_D = \frac{\pi\sqrt{\varepsilon_{r\ dyn}\left(\varepsilon_r, h, 2r_o\right)}}{\lambda_0\,\alpha_d} \tag{8}$$

The dielectric loss, α_d is determined from the standard expression. The free-space wavelength (λ_0) is obtained from the resonance frequency of the patch. It is determined for the loss-less substrate i.e., $\tan\delta_{eff} = 0$ by the equation (1). The Q_C is also computed for the equivalent rectangular patch of width, $W = 2r_o$ from,

$$Q_C = \frac{\pi\sqrt{\varepsilon_{r\ dyn}\left(\varepsilon_r, h, 2r_o\right)}}{\lambda_0\left(\alpha_c + \alpha_{feed}\right)} \tag{9}$$

The α_c is the conductor loss of the patch and ground plane taken together and is determined by the Wheeler's inductance rule, which has been adopted by Verma et al. [15] in the variational method. The α_{feed} is loss in the probe feed, which is determined by following the method of Collin [16].

To compute Q_R due to the radiation loss, we have adopted two methods. In the model one, called MWM1 the Q_R is computed for the equivalent rectangular aperture of width, $W = 2r_o$. The expressions are summarized in the reference [17]. For the model-2 i.e. for the MWM2, the Q_R is computed for the circular aperture of the cavity resonating in the TM_{11} mode. The Q_R for the circular aperture used in the MWM2 is [14],

$$Q_R = \frac{4r_o\left(\alpha_{11}^2 - 1\right)\varepsilon_{r\,dyn}^{3/2}}{h\,\alpha_{11}^3 F\left(\alpha_{11}\big/\sqrt{\varepsilon_{r\,dyn}}\right)} \tag{10}$$

The function F(X), where $X = \dfrac{\alpha_{11}}{\sqrt{\varepsilon_{r,dyn}}}$ is given by the following approximate expression,

$$\begin{aligned} F(X) = {} & 2.666667378 - 1.066662519X^2 + 0.209534311X^4 - 0.019411347X^6 \\ & + 0.001044121X^8 - 0.000049747X^{10} \end{aligned} \tag{11}$$

Finally, Q_{SW} due to the surface-wave loss is obtained from,

$$Q_{sw} = Q_r\frac{P_{sp}}{P_{sw}} \tag{12}$$

The radiated power i.e. power in the space wave (P_{sp}) and power in the surface waves (P_{sw}) are obtained from the closed-form expressions due to Pozar [18]. From the total Q- factor we find the effective loss tangent, $\tan\delta_{eff}$ of the substrate,

Copyright SBMO ISSN 1516-7399

$$\tan\delta_{eff} = \frac{1}{Q_T} \tag{13}$$

At this stage, the complex relative permittivity of the substrate is taken as $\varepsilon_r^* = \varepsilon_r' - j\varepsilon_r' \tan\delta_{eff}$. This is used for computation of the complex dynamic relative permittivity $\varepsilon_{r,dyn}^*$ of the circular patch and finally loss dependent resonance frequency by the equation (1). However, the decrease in the resonance frequency due the surface wave and radiation losses is meaningful only when the substrate thickness is more $0.1\lambda_g$. For the substrate thickness $0.22\lambda_g$ decrease in resonance frequency due to the surface wave and radiation losses is about 3% [19].

The inductive reactance of probe, X_L indicating effect of all non-resonating modes is given by [19],

$$X_L = \frac{377 f h}{v_0} \log\left[\frac{v_0}{\pi f d_o \sqrt{\varepsilon_{req}'}}\right] \tag{14}$$

where, f is the operating frequency.

III. RESULTS AND DISCUSSION

The Table 1(a) shows the experimental results on the resonance frequency and the input resistance (R_{max}) of seventeen circular patches in the substrate thickness range from $0.003\lambda_g$ - $0.1\lambda_g$ [2-8]. The Table 1(b) and the Table 1(c) compare three commercial software and the MWM against the experimental resonance frequency and the experimental input resistance respectively. Both the tables clearly demonstrate that the present MWM is much better than all three models of the commercial software. The MWM has maximum deviation within 1.69 % and 17% for the resonance frequency and the input resistance respectively. Other three models provide the deviation above 5% for the resonance frequency and the deviation between 35% - 55% for the input resistance. Only patch numbers 3 and 9 show inconsistent results. For input resistance, the MWM2 shows better agreement with the experimental results as compared to the MWM1. For the MWM1, Q_R is computed for the equivalent rectangular aperture of width, $W = 2r_o$, whereas for the MWM2, the Q_R is computed for the circular aperture of the cavity resonating in the TM_{11} mode.
The Table 2 further compares the total Q- factor (Q_T) and the bandwidth computed by the mode matching method (MMT), MWM1 and MWM2 against the experimental results for the patch numbers 12,14, and 16. For these patches the bandwidth is defined for VSWR < 1: 3 [2]. The results for Q_T obtained by the MMT closely follow results of the MWM1. However, for the bandwidth, the MWM2 shows better agreement with experimental results. It appears that the deviation in bandwidth and Q_T computed by the MWM from the experimental results is due to the fact that the expression of Pozar [18] for the surface wave loss is applicable to the conductor backed infinite dielectric medium not to the finite size case of microstrip antenna. This has given approximate results on the Q-factor due to the surface wave loss.

Fig. 2 further compares the normalized real and imaginary parts of input impedance of the thick circular patch number 16 computed by MWM2, MMT and MOM based Ensemble against

Copyright SBMO ISSN 1516-7399

the experimental results. The results of MWM2 and MMT show better agreement with the experimental results as compared to the results of Ensemble.

Table 1(a): Experimental Results of Resonance Frequency (f_r) and Input Resistance (R_{max}).

Ref.	Patch No.	h (mm)	h/λ_g	r_o (mm)	ρ (mm)	ε_r	tanδ	f_r (GHz)	R_{max} (Ω)
[3]	1	0.800	0.003	68.00	65.0	2.32	0.001	0.835	153.5
	2	1.590	0.007	68.00	65.0	2.32	0.001	0.829	242.0
	3	3.180	0.013	68.00	65.0	2.32	0.001	0.815	256.0
[4]	4	1.590	0.010	50.00	47.5	2.32	0.001	1.128	400.0
[5]	5	1.524	0.012	38.0	11.7	2.49	0.001	1.443	66.0
[6]	6	1.5875	0.011	41.91	10.2	2.50	0.002	1.314	45.0
	7	3.175	0.022	41.91	11.4	2.50	0.002	1.286	69.0
[7]	8	1.600	0.024	14.10	14.1	2.58	0.001	2.830	352.0
[8]	9	0.350	0.005	18.90	18.9	2.47	0.001	2.885	147.0
	10	0.750	0.011	18.90	18.9	2.47	0.001	2.860	310.5
	11	1.600	0.024	18.90	18.9	2.47	0.001	2.810	437.0
[2]	12	1.600	0.030	14.10	7.5	2.62	0.001	3.540	191.0
	13	1.600	0.030	14.10	10.5	2.62	0.001	3.540	270.0
	14	3.200	0.060	13.50	7.6	2.62	0.001	3.600	165.0
	15	3.200	0.060	13.50	10.5	2.62	0.001	3.600	245.0
	16	4.700	0.090	13.00	7.5	2.62	0.001	3.50	175.0
	17	4.700	0.090	13.00	10.5	2.62	0.001	3.50	270.0

Table 1(b) : Computed Resonance Frequency (f_r) and % Deviation from Experimental Results.

Patch No.	Ensemble [9]		PCAAD [10]		MCM [11]		MWM	
	f_r GHz	% Dev.	f_r GHz	% Dev.	f_r GHz	% Dev.	f_r GHz	% Dev.
1	0.798	4.43	0.839	-0.48	0.839	-0.48	0.836	-0.12
2	0.793	4.34	0.832	-0.36	0.835	-0.72	0.830	-0.12
3	0.783	3.93	0.822	-0.86	0.820	-0.61	0.819	-0.49
4	1.155	-2.39	1.126	0.18	1.126	0.18	1.126	0.18
5	1.444	-0.07	1.426	1.18	1.427	1.11	1.440	0.21
6	1.308	0.46	1.292	1.67	1.318	-0.30	1.310	0.30
7	1.284	0.16	1.268	1.40	1.270	1.24	1.280	0.47
8	2.840	-0.35	2.776	1.91	2.780	1.77	2.830	0.00
9	2.985	-3.47	2.914	-1.00	2.920	-1.21	2.890	-0.17
10	2.945	-2.97	2.878	-0.63	2.880	-0.70	2.870	-0.35
11	2.875	-2.31	2.817	-0.25	2.820	-0.36	2.802	0.29
12	3.725	-5.23	3.635	-2.68	3.640	-2.82	3.600	-1.69
13	3.725	-5.23	3.635	-2.68	3.640	-2.82	3.600	-1.69

Copyright SBMO ISSN 1516-7399

14	3.650	-1.39	3.653	-1.47	3.660	-1.67	3.560	1.11
15	3.625	-0.69	3.653	-1.47	3.660	-1.67	3.560	1.11
16	3.575	-2.14	3.683	-5.23	3.700	-5.71	3.505	-0.14
17	3.475	0.71	3.683	-5.23	3.700	-5.71	3.505	-0.14
Max. % Dev.		-5.23	-5.23		-5.71		-1.69	
Average % Dev.		-0.72	-0.94		-1.20		-0.07	
RMS % Dev.		0.72	0.55		0.58		0.18	

Table 1(c): Computed Maximum Resonant Resistance (R_{max}) in Ohms and % Deviation from Experimental Results:

Patch No.	Ensemble [9]		PCAAD [10]		MCM [11]		MWM1		MWM2	
	R_{max}	Dev.	R_{max}	Dev.	R_{max}	Dev.	R_{max}	Dev.	R_{max}	Dev.
1	193.0	-25.7	119.1	22.4	168.0	-9.4	176.4	-14.9	175.9	-14.6
2	320.9	-32.6	235.6	2.6	235.0	2.9	277.0	-14.5	276.6	-14.3
3	383.9	-50.0	314.0	-22.7	358.6	-40.1	338.6	-32.3	333.6	-30.3
4	335.8	16.1	274.8	31.3	329.6	17.6	358.9	10.3	355.6	11.1
5	78.9	-19.5	72.6	-10.0	75.8	-14.8	73.7	-11.7	71.2	-7.9
6	45.2	-0.4	42.8	4.9	46.4	-3.1	46.6	-3.6	45.0	0.0
7	61.0	11.6	67.0	2.9	63.7	7.7	64.4	6.7	61.5	10.9
8	309.1	12.2	330.0	6.3	337.0	4.3	346.9	1.4	324.6	7.8
9	215.6	-46.7	136.6	7.1	183.5	-24.8	203.2	-38.2	201.9	-37.3
10	308.6	0.6	265.9	14.4	335.5	-8.1	334.7	-7.8	324.1	-4.4
11	359.5	17.7	343.3	21.4	406.0	7.1	416.7	4.6	360.5	17.5
12	180.5	5.5	227.0	-18.8	215.0	-12.6	218.3	-14.3	201.6	-5.5
13	295.5	-9.4	339.8	-25.9	339.5	-25.7	332.8	-23.3	307.4	-13.9
14	210.3	-27.5	260.5	-57.9	224.6	-36.1	207.4	-25.7	189.9	-15.1
15	324.8	-32.6	371.2	-51.5	346.2	-41.3	303.4	-23.8	277.9	-13.4
16	231.3	-32.2	272.8	-55.9	218.1	-24.6	189.0	-8.0	170.2	2.7
17	364.6	-35.0	384.6	-42.4	341.0	-26.3	278.2	-3.0	250.5	7.2
Average % Dev.		-14.6	-10.1		-13.4		-11.6		-5.8	
RMS % Dev.		6.4	7.2		5.3		4.3		3.8	

Table 2: Comparison of Total Q-Factors and Bandwidth [2]

Patch No.	Q factor MMT [2]	% Bandwidth (VSWR < 3:1) Expt. [2]	% Bandwidth (VSWR < 3:1) MMT [2]	Q factor		% Bandwidth	
				MWM 1	MWM2	MWM 1	MWM 2
12	33.0	5.0	3.5	35.6	30.3	3.3	3.9
14	15.0	10.0	7.7	15.4	13.3	7.5	8.7
16	9.0	18.0	12.8	9.2	8.0	12.6	14.4

Copyright SBMO ISSN 1516-7399

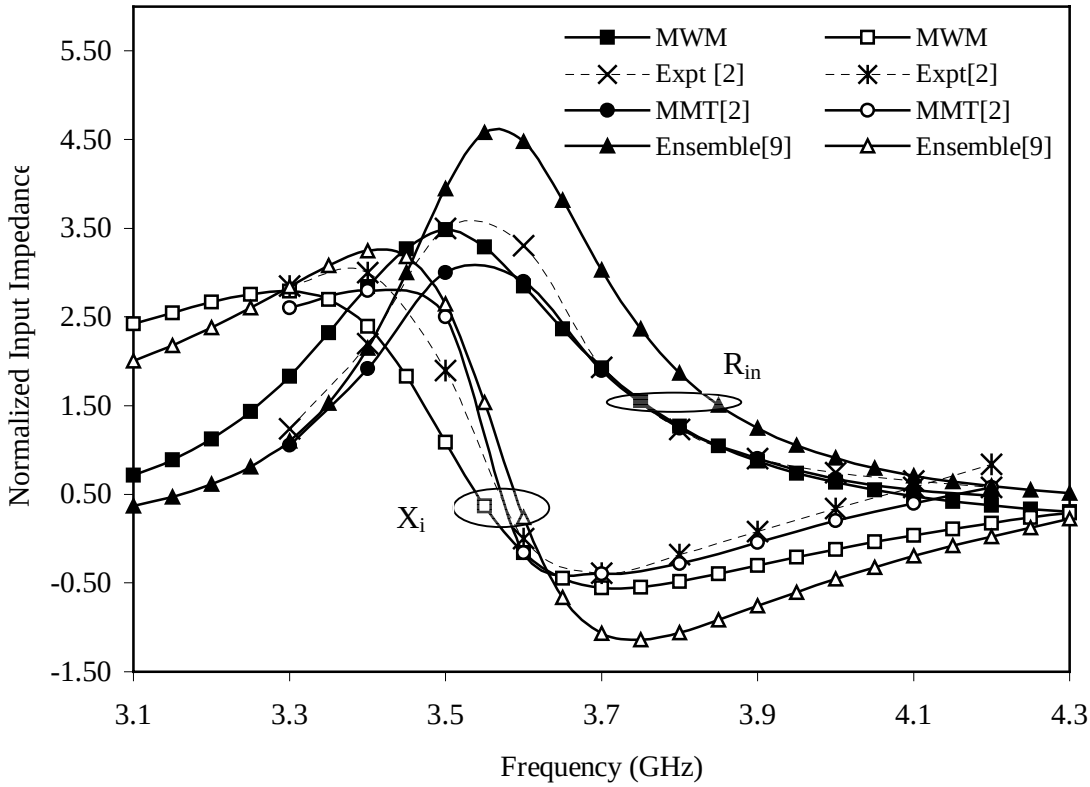

Fig. 2. Normalized Input Impedance of circular patch on thick substrate for the patch no. 16.

IV. CONCLUSION

The MWM based cavity model for the circular patch antenna has better accuracy than accuracy of the three considered commercial software. Following the previous investigation on the multilayer rectangular microstrip patch antenna [20], the present model can be extended to a circular microstrip patch antenna under the multilayer condition. The present MWM is flexible, accurate and computationally faster compared to the field theoretic methods like MOM and MMT. Therefore, the present MWM is suitable for the interactive CAD.

REFERENCES

[1] A.K. Verma and Z. Rostamy, "Modified Wolff Model for determination of resonance frequency of dielectric covered circular microstrip patch antenna," *Electronics Letters*, Vol. 27, pp. 2234-2236, Nov. 1991.

[2] M. Davidovitz and Y. T. Lo, "Input Impedance of a Probe-fed circular microstrip antenna with thick substrate," *IEEE Trans. on Antennas and Propagation*, Vol. AP-34, No. 7, pp. 905-911, July 1986.

Copyright SBMO ISSN 1516-7399

[3] J. S. Dahele and K. F. Lee, "Effect of Substrate Thickness on the performance of Circular-Disk Microstrip Antenna," *IEEE Trans. on Antennas and Propagation*, Vol. AP-31, pp. 358-360, March 1983.
[4] J. S. Dahele and K. F. Lee, "Theory and Experiment on Microstrip Antenna with air gaps," *IEE, Proc*., Vol.132, Pt. H, pp. 455-460, Dec.1985.
[5] K.R. Carver, "Practical analytical techniques for the microstrip antenna," *Proc. Workshop on Printed Circuit Antenna Technology*, 17-19 Oct.1979, New Mexico State University, Las Cruces, New Mexico, pp. 7-1-20.
[6] S. Yano and A. Ishimaru, "A Theoretical Study of the Input Impedance of a Circular Microstrip Disk Antenna," *IEEE Trans. on Antennas and Propagation*, Vol. AP-29, pp. 77-83, Jan.1981.
[7] W. C. Chew and J. A. Kong, "Analysis of a circular Microstrip Disk Antenna with a thick Dielectric Substrate," *IEEE Trans. on Antennas and Propagation*, Vol. AP-29, pp. 68-76, Jan.1981.
[8] S. A. Long, L. C. Shen, M. D. Walton and M. R. Allerding, "Impedance of a Circular Disk Printed–Circuit Antenna," *Electronics Letters*, Vol. 14, pp. 684-686, Oct.1978.
[9] Ensemble Version 6.1, Ansoft Co., USA, Sept. 1999.
[10] D. M. Pozar, PCAAD 3.0, Personal Computer Aided Antenna Design, Antenna Design Associates, Inc. 1996.
[11] A. Benalla, C. H. Thng and K. C. GUPTA, Computer-Aided design and analysis of microstrip patch antennas', Micropatch Version 2.0, 1993.
[12] R. Garg, P. Bhartia, I. Bahl, A. Ittipiboon, Microstrip Antenna Design Handbook, Artech House, Inc., 2001, pp. 366.
[13] W. C. Chew, and J. A. Kong, "Effects of fringing fileds on the capacitance of circular microstrip disk," *IEEE Trans., Microwave Theory Tech*., Vol. 26, no. 2, pp. 98-103, 1980.
[14] F. Abboud, J. P. Damiano, and A. Papiernik, "A new model for calculating the input impedance of coax-fed circular microstrip antennas with and without air gaps," *IEEE Trans. Antennas Propagat*., vol. AP-38, pp. 1882-1885, Nov. 1990.
[15] A. K. Verma and A. Bhupal, 'Conductor loss of multilayer microstrip line using single layer reduction formulation', *Microwave Opt. Technol. Lett*., Vol.19, No.1, pp. 20-24, 1998.
[16] R. E. Collin, Antennas and Radiowave propagation, McGraw-Hill, New York, 1985, pp. 273-283.
[17] J. R. James and A. Henderson, and P. Hall "Microstrip antenna performance is determined by substrate constraints," *MSN*, pp. 73-83, August 1982.
[18] D. M. Pozar, "Rigorous closed-form expressions for the surface wave loss of printed antennas," *Electron. Lett*., Vol. 26, No.13, pp. 954-956, 1990.
[19] A. K. Verma and Nasimuddin, "Resonance frequency of rectangular microstrip antenna on thick substrate," *Electron. Lett*, Vol. 37, No. 23, pp. 1373-1374, Nov. 2001.
[20] A. K. Verma and Nasimuddin, "Input Impedance of Rectangular Microstrip Patch Antenna with Iso/Anisotropic Substrate-superstrate," *IEEE Microwave and Wireless Components Letters*, Vol. 11, No. 11, Nov. 2001.

Copyright SBMO ISSN 1516-7399